




# Diffusion mediated rigidity-gradient hydrogel substrate for cellular mechanosensing

Indrajit Bhattacharjee<sup>1</sup>, Sukanya Sudhiram<sup>1</sup>, M. Nithya<sup>2</sup>, Bharat Kumar<sup>2</sup>, and Bibhu Ranjan Sarangi<sup>1,3,a</sup> 

<sup>1</sup> Physical and Chemical Biology Lab, Department of Physics, Indian Institute of Technology Palakkad, Palakkad, Kerala 678623, India

<sup>2</sup> Department of Physics, Central University of Karnataka, Kadaganchi, Karnataka 585367, India

<sup>3</sup> Department of Biological Sciences and Engineering, Indian Institute of Technology Palakkad, Palakkad, Kerala 678623, India

Received 6 December 2023 / Accepted 16 February 2024

© The Author(s), under exclusive licence to EDP Sciences, Springer-Verlag GmbH Germany, part of Springer Nature 2024

**Abstract** Mechanical cues in the cellular micro-environment play pivotal role in several important biological processes. The rigidity of the substrate has been shown to dictate the cellular morphology through the reorganization of the actin cytoskeleton. Substrates with spatially varying rigidity are most often used to investigate the coupling of the substrate rigidity and intracellular mechanosensing machinery. Here, we present a simple yet effective method for producing hydrogel substrates with a tunable rigidity gradient. Using atomic force microscopy and epifluorescence microscopy, we have characterized the substrate in terms of rigidity. Furthermore, we have investigated the cellular response on these substrates with spatially varying rigidity.

## 1 Introduction

Cells have the ability to sense and respond to mechanical cues from their micro-environment. In particular, the rigidity of the extracellular matrix has been shown to play a crucial role in various processes both at the level of cells and tissues. Cell migration, differentiation, proliferation, development, and disease progression are some of the processes related to rigidity sensing [1–5]. At the level of individual cells, substrate rigidity can influence cell morphology, structure of actin cytoskeleton, polarization, and movement of the cell [6–8]. With increasing substrate rigidity, the actomyosin network tends to become more ordered and the morphological characteristics of the cell change from that of a nearly circular shape to a more elongated shape. The adhesion area also increases as the rigidity increases [9]. When presented with a rigidity gradient, cells have been shown to move toward the stiffer region of the substrate [10].

Hydrogels are one of the promising materials that have been extensively used for investigating cell substrate interaction. Hydrogel is a type of polymer network that swells in water and has a three-dimensional network structure. They have adjustable physicochemical qualities that may be tuned to meet the experimental needs specifically in terms of mechanical properties. Physical or chemical cross-linking methods have the potential to modify the mechanical properties of hydrogels. Physical cross-linking, which involves hydrophobic interactions, hydrogen bonding, polymerisation entanglement, etc., typically results in weak mechanical strength. However, covalent cross-linking, such as free radical polymerisation and enzyme-induced cross-linking, leads to high mechanical strength [11]. Synthetic bio-compatible peptide-polymer conjugate network with tunable stiffness was recently shown to mimic the actomyosin network present in cells [12].

Several methods have been employed to create a rigidity gradient substrate to investigate both the individual and the collective response of cells. One of the simplest ways to create a rigidity gradient is by mixing hydrogel solutions to create a concentration gradient induced rigidity variation. Microfluidic devices have been used to facilitate the mixing of hydrogel solutions with varying concentrations, allowing the creation of substrates with stiffness gradients [13, 14]. Controlled diffusion has also been used to create a gradient [15]. However, most of these methods require complex experimental procedures and often lack the tunability.

<sup>a</sup> e-mail: [bibhu@iitpkd.ac.in](mailto:bibhu@iitpkd.ac.in) (corresponding author)

Polyacrylamide (PAA) hydrogel is frequently used for the fabrication of rigidity-gradient substrates owing to the availability of simple methods to modify its stiffness using both composition and external parameters such as light intensity and exposure duration when using a photo-initiator facilitated cross linking. The achievable value of rigidity is in the range of a few kPa to several hundred kPa. Here, we report a simple procedure for creating a stiffness gradient by mixing PAA hydrogel solutions. Using combinations of hydrogels with different stiffnesses, we demonstrate an optimum way to obtain a high stiffness gradient. We have characterized the substrate both by fluorescence imaging and by atomic force microscopy for mechanical characterization. We also show the morphological variation of cells on such a substrate.

## 2 Experimental section

### 2.1 Hydrogel substrate preparation

The chamber for the hydrogel mixing was prepared using polydimethylsiloxane (PDMS) (Sylgard 184, Sigma-Aldrich) [16]. An appropriate amount of the mixture (base and curing agent) was poured into a petridish to produce a PDMS sheet of approximately 1 mm thickness. After degassing, the mixture was cured in an oven at 60 °C for 3 h. A rectangular chamber with dimensions of 15 mm × 5 mm was cut from the prepared PDMS sheet. Aminosilanated coverslips were prepared to attach the polyacrylamide gel. The coverslips were first washed with 70% ethanol solution. 0.1 nM NaOH solution was poured on top of the coverslips and heated to 80 °C on the hot plate. 3-Aminopropyltriethoxysilane (Sigma-Aldrich) was added to the coverslips and kept for 5 min. The coverslips were then thoroughly washed with deionized water. Finally, 0.5% (v/v) glutaraldehyde in phosphate-buffered saline (Sigma-Aldrich) was added. After 30 min, the coverslips were air-dried. Dichlorodimethylsilane (Sigma-Aldrich) was used to make a chlorosilanated coverslip that was used as the top cover of the chamber containing PAA gel [17]. The coverslip was treated with dichlorodimethylsilane and left to react for 5 min. Then, it was submerged in water for 1 min and air-dried at room temperature. To prepare the mold, we placed the PDMS chamber on the aminosilanated coverslip. The PDMS chamber was cut into two equal parts with a tiny gap. The chlorosilanated coverslip was then placed on top of the chamber to create a confined space. A schematic of the PDMS chamber is shown in Fig. 1a.

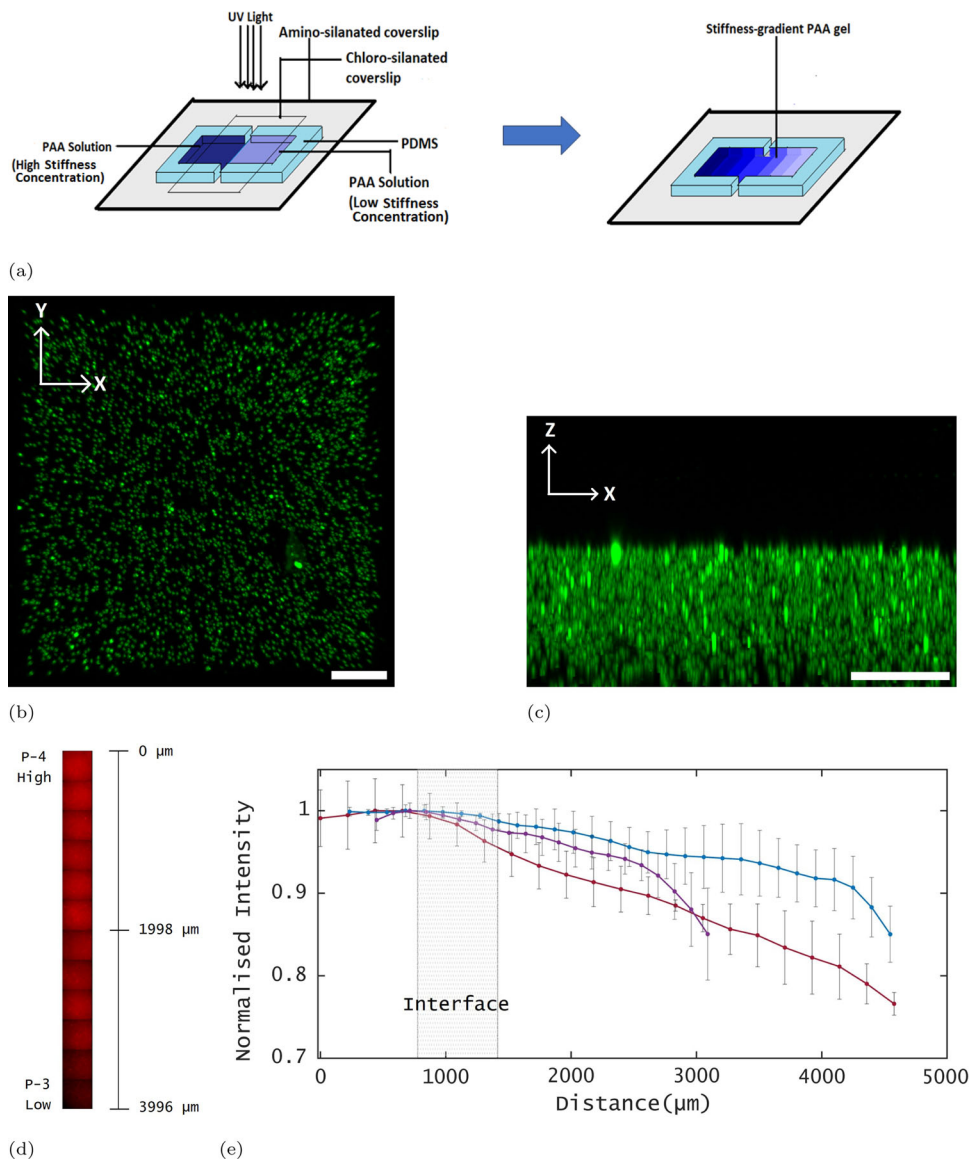
Polyacrylamide solutions were prepared using combinations of acrylamide monomer (Sigma-Aldrich) and bis-acrylamide (Sigma-Aldrich) at varying concentrations to produce the desired substrate rigidity. We have used specifically four combinations which we refer to as P-1 (acrylamide 4% + bis-acrylamide 0.1%), P-2 (acrylamide 5% + bis-acrylamide 0.1%), P-3 (acrylamide 8% + bis-acrylamide 0.48%), and P-4 (acrylamide 12% + bis-acrylamide 0.25%). To photopolymerize the hydrogel solution, Irgacure 2959 (Sigma-Aldrich) was used at a concentration of 0.5 mg/ml. With the specified combinations, P-4 is supposed to give the highest rigidity value among the four and P-1 the lowest. P-2 and P-3 are expected to have rigidity values between P-1 and P-4 [17, 18]. All four substrates were characterized by atomic force microscopy for rigidity.

The polymerisations of the prepared solutions were carried out in the PDMS chamber. First, half of the chamber was filled with a higher rigidity solution for a particular combination. The lower stiffness solution was slowly added from the other side of the chamber, so that the solution gradually approached the interface of the higher stiffness solution. After allowing it to stabilize for 30 s, the system was exposed to a 15 watt UV lamp for 6 min. Typically, 3–4 min of UV exposure is sufficient to complete hydrogel photopolymerisation [18, 19]. Subsequently, the top cover was carefully removed to maintain the smoothness of the surface. The sample was immersed in deionized water for a duration of 10 min to remove any unpolymerized acrylamide monomer that may be left in the gel.

To gain an understanding of the simultaneous processes of diffusion and polymerisation, we allowed various combinations of polymerising solutions (corresponding to different rigidity) to diffuse into each other in the prepared PDMS chamber. TetraSpeck beads (Thermo Fisher Scientific) of 250 nm size were used to track the polymerisation-inhibited mixing process.

Beads in fixed concentration were added to the higher rigidity pre-polymerisation solution. The chamber was fixed to a rectangular coverslip. Half of the chamber was then filled with the higher rigidity solution. The lower rigidity solution is then slowly added in the other half, so that the solutions gradually meet at a region marked as the interface. The diffusion is allowed to take place for 30 s, after which the system is illuminated by UV light for 6 min to facilitate photopolymerisation. The synthesized hydrogel samples were then imaged using fluorescence microscopy. Average intensity profiles of the beads were plotted from the set of three measurements for each set of combinations. The substrates were also imaged using confocal microscope for probing the surface characteristics. The surface was observed to be homogeneous coarse grained over a length scale bigger than the bead size. The top view and side view of a representative substrate is given in Fig. 1b and c.

**Fig. 1** **a** Schematic diagram of the experimental setup. The left side of the image shows the hydrogel mixing chamber and the right side represents the substrate after polymerisation under UV light. The color gradient is used to indicate the variation of stiffness across the substrate. **b** and **c** Confocal microscopy image showing top and cross-sectional view of the substrate. **d** An epifluorescence microscope image of a substrate showing the intensity variation due to the distribution of fluorescent beads throughout the sample (combination P-4 and P-3). **e** Spatial intensity distribution plot for various combinations of polymer solutions—the blue curve (P-3 and P-2), purple curve (P-4 and P-3), and red curve (P-4 and P-1) represent the corresponding intensity distributions obtained from mixed samples. Scale bars = 50  $\mu\text{m}$



## 2.2 Atomic force microscopy on the hydrogel substrate

The gradient in the elastic moduli on the samples is measured using atomic force microscopy (CS Instruments, Model: Nano Observer). V-shaped silicon nitride contact mode cantilevers (Budget Sensors) of spring constant 0.06 mN/m were used for the indentation studies. The force–distance curves ( $F$ – $d$  curves) were obtained in the liquid medium for different hydrogel samples. The indentation depth ( $\delta$ ) in the samples for different forces was calculated and the  $F$  –  $\delta$  plots were analyzed applying the Hertzian model. The radius of the tip for the AFM cantilevers used was 15 nm. A typical  $F$ – $d$  curve obtained in the contact mode is shown in Fig. 2. For a parabolic indenter, the Hertzian model specifies the following relation between the force and the indentation ( $\delta$ ) as given below [20]:

$$F = \frac{4E}{3(1 - \nu^2)} \sqrt{R\delta^3}. \tag{1}$$

Here,  $E$  is the elastic modulus,  $R$  is the radius of the AFM tip, and  $\nu$  is the Poisson ratio for the sample, which is taken to be 0.5. The indentation depth is calculated by  $\delta = d - D$ , where  $d$  is the sample displacement and  $D$  is the deflection of the cantilever. Elastic moduli  $E$  for different positions on the sample were obtained by averaging multiple ( $\sim 10$ ) indentation on the sample. The plot of  $E$  as a function of position is shown in the Fig. 2 for different samples. The error bars denote standard deviation.

### 2.3 Substrate functionalization

To promote cell adhesion, we use succinimide cross-linking mediated by sulfo-SANPAH for the covalent attachment of fibronectin to PAA hydrogels [21]. Briefly, the prepared hydrogel was placed in a 35 mm petridish and Sulfo-SANPAH (0.2 mg/ml in HEPES with a pH of 8.5) was added. The substrate was then exposed to UV light for 20 min to facilitate the reaction. It was followed by washing with 50 mM HEPES to remove excess Sulfo-SANPAH. The same process was repeated to ensure optimal protein binding. Subsequently, the substrate was incubated with 50  $\mu$ l of bovine plasma fibrin (Thermo Fisher Scientific) at 37 °C for 5 h. Previous studies have shown that incubation of protein solutions at a concentration of 0.1 mg/ml for 30 min results in the achievement of saturated levels of adhesion proteins on hydrogels, regardless of substrate stiffness [22]. The substrate was thoroughly rinsed with HEPES solution to remove excess fibronectin. The mixture was then immersed in 1X PBS and stored at a temperature of 4 °C for future use.

### 2.4 Cell culture

3T3 cells were exposed to the functionalized stiffness gradient substrate to investigate the mechanical response of the cells to different stiffness. Cell culture media was constructed with DMEM along with 10% fetal bovine serum (HIMEDIA) and w/80U penicillin, 80  $\mu$ g streptomycin, and 0.2  $\mu$ g amphotericin B in per ml, and cells were incubated at 37 °C with 5% CO<sub>2</sub>. The cells were cultivated for a period of 2 days before seeding on the substrate. They were then seeded on the stiffness gradient substrate at a density of typically 35 cells /mm<sup>2</sup>.

### 2.5 Cell staining

Following a 48-h incubation period, cells were fixed with 4% paraformaldehyde for 30 min at room temperature. Subsequently, they were rinsed three times for 5 min each with 1X PBS, which included 0.05% Tween-20. The cells were then permeabilized with 0.3% Triton X-100 for 15 min at room temperature, followed by another three washes with 1X PBS (0.05% Tween-20). To stain the cell nuclei, DAPI (4',6-diamidino-2-phenylindole) (Sigma-Aldrich) was used at a concentration of 1  $\mu$ g per ml in 1X PBS for 5 min, followed by three additional washes with 1X PBS (0.05% Tween-20). For f-actin staining, ActinRed™ 555 ReadyProbes™ Reagent (containing Rhodamine phalloidin from Thermo Fisher Scientific) was used, with an incubation period of 1 h and again three washes with 1X PBS (0.05% Tween-20). Focal adhesions within cells were stained with vinculin (FAK100, Sigma-Aldrich).

### 2.6 Microscopy and image analysis

The samples obtained from the diffusion assay were imaged using fluorescence microscopy (Olympus IX83) under the TRITC filter. Images were acquired with 40  $\times$  resolution along horizontal strips on the gel. The average intensity of a region of around 0.01 mm<sup>2</sup> was measured in individual images. The intensity data (obtained using ImageJ) were smoothed out by taking sliding average for each data set. Average curves are obtained from such measurements. The error bars correspond to standard deviation of the data. Figure 1e shows the averaged curves plotted for three combinations. The confocal microscopy images were obtained using OLYMPUS FV3000 confocal microscope. A bead-embedded sample (P-3 with P-2) was captured using the 10  $\times$  air objective. The scanning area was typically 323.9  $\mu$ m by 323.9  $\mu$ m, with a Z dimension of 145  $\mu$ m having a Z spacing of 1  $\mu$ m.

To quantify the extent of cell spreading and changes in cell shape in response to variations in substrate stiffness, the experimental procedure involved observation of cells using phase contrast microscopy, as well as the use of DAPI and TRITC filters of the fluorescence microscope (Olympus IX83 U-LH100L-3). The observations were made using a 10  $\times$  air objective. Image acquisition was accomplished by displacing the motorized XY stage of the microscope by a magnitude of 1 mm along the X and Y axes in both positive and negative directions. In this manner, complete images of the samples were captured. To examine the establishment of cell focal adhesion and f-actin in response to varying substrate stiffness, we used a confocal microscope (OLYMPUS-FV3000).

Image analysis was performed using open source software ImageJ software (National Institutes of Health, USA). After suitable thresholding of image stacks, the region of cell spreading was detected using the particle analysis plugin. Furthermore, the circularity of the cell was also measured, where circularity is defined as circularity =  $4\pi \frac{\text{area}}{\text{perimeter}^2}$ . We have analyzed a minimum of 100 cells per condition with a total of more than 1200 individual cells over different stiffness areas of the substrates to quantify the variation of the cell's spreading area and cell shape (circularity) as a function of the variation in stiffness of the substrate. Standard deviation of the data was used to plot the error bars.

### 3 Results and discussion

#### 3.1 Mixing induced gradient

Fluorescent beads are used to track the diffusion of the polymer solution with higher rigidity into that with lower rigidity. They serve as better tracers compared to molecular tracers such as rhodamine dye, as the movements of the beads are expected to be influenced only by the hydrogel structure [23]. The underlying assumption here is that the beads do not show independent diffusion; rather, they diffuse with the polymer solution. Furthermore, the bead size is significantly larger than the hydrogel mesh size distribution [24]. Thus, once the hydrogel network is formed, it will hinder the movement of the beads considerably.

In the samples obtained from the diffusion assay, the bead distribution and hence the intensity are therefore expected to bear the signature of the concentration distribution of the higher rigidity polymer solution. It is evident from the intensity analysis of the bead distribution that concentration gradient-driven diffusion is arrested by polymerisation. Prior to the completion of the polymerisation process, diffusion creates a concentration gradient of the high-rigidity polymer solution in the lower rigidity solution. On completion of polymerisation, a gradient in rigidity emerges near the interfacial region. The intensity plot (Fig. 1e) reflects this phenomenon. The decay profiles for the various combinations look similar. This may possibly arise as a result of two processes, namely diffusion and polymerisation. Diffusion occurs over longer time scales and only in pre-polymerised solutions. Once polymerisation has occurred, the beads are no longer able to diffuse freely. Polymerisation happens at a much faster time scale and depends on the duration and intensity of exposure to UV for a fixed concentration of cross-linker and photoinitiator. Thus, the intensity curves for all three combinations may show similar decay profile.

Another discernible feature of the plot is that the penetration length of the higher rigidity solution is minimum for the combination of P-4 with P-3. This can be attributed to the fact that when polymerisation takes place, the cross-linking density would be highest in this combination compared to P-4 with P-1 or P-3 with P-2.

#### 3.2 Stiffness gradient measurement

To attain a tunable stiffness gradient on the substrate, different combinations of the polyacrylamide solutions as mentioned above were used. Figure 2a shows a typical  $F - \delta$  curve for the diffusion sample of P-4 and P-3. The inset shows the  $F - d$  curve. The solid line is a fit to the data according to Eq. (1). Elastic moduli for different positions on the sample were obtained from the fit parameters. The plot of  $E$  as a function of position is shown

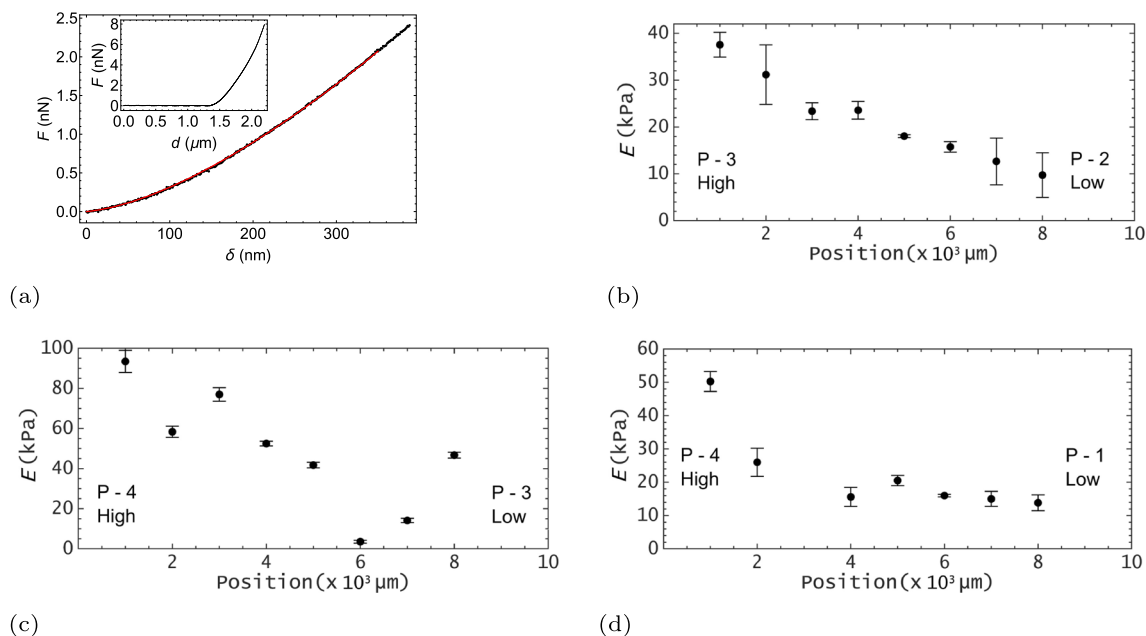


**Fig. 2** Mechanical characterization of the substrates by Atomic Force Microscopy: **a** One of the example of  $F - d$  curve obtained in contact mode (combination P-4 with P-3). The inset shows a typical  $F - d$  curve for the sample of diffusion between P-4 and P-3. The solid line is a fit to the data as per the equation 1. **b–d** depict the variation in rigidity observed across the substrates when combining hydrogels P-3 with P-2, P-4 with P-3, and P-4 with P-1, respectively. Error bars represent the standard deviation

in Fig. 2b–d for different samples. The measured values of the elastic moduli are close to the values reported previously [17]. The deviation of the rigidity values may possibly arise from the fact that the rigidity is a function of the cross-linking density. Since we make use a photoinitiator for polymerisation, the intensity of UV light as well as the duration of exposure will dictate the cross-linking density. Therefore, the obtained rigidity values will be more sample-specific. Figure 2 illustrates how varying the combination of polyacrylamide solutions can alter the substrate stiffness gradient. In the context of the combination of polyacrylamide solutions, such as the combinations P-3 with P-2, P-4 with P-3, and P-4 with P-1, we observed changes in rigidity ranging from 37.5 to 9.75 kPa, 93.4 to 40.6 kPa, and 50.2 to 11.2 kPa, respectively, across the substrates (Fig. 2b–d). The experimental setup involved the use of a combination of P-4 with P-4 as control. In this case, the substrate does not have a stiffness gradient and the results obtained yielded an average stiffness value of around  $(72 \pm 6)$  kPa. Other combinations of hydrogel solutions yield various ranges of rigidities (see supplementary information).

The values of the rigidity gradient were estimated for different combinations of hydrogel preparations (see Supplementary Table 1). One important aspect of our observation is the length scales over which these rigidity variations are observed varies for different combination. For example for the combination of P-4 with P-1, a gradient of 15 kPa/mm was found over 3 mm over the substrate near the interfacial region. The values obtained for the rigidity gradient of the substrates are consistent with those previously reported [15, 25]. However, the intensity data from fluorescence microscopy do not provide an absolute correlation with that of rigidity gradient as measured by AFM. As explained previously, different combinations show a similar decay profile in intensity. However, the bead distribution helps to visualize the concentration gradient of the higher rigidity solution in the lower rigidity solution and hence the extent of mixing of the two polymer solutions.

### 3.3 Cellular response on gradient substrate

We used 3T3 fibroblast cells to investigate the cellular mechanosensing in response to the stiffness variation of the substrate. To obtain optimum response to the variation of the stiffness of the substrate, we used a combination of hydrogels that have the highest possible stiffness variation in the range of 12–50 kPa over a relatively small spatial distance (Fig. 3a) shows the epifluorescence images of cells seeded on the gradient substrate. Images of cells taken at different locations corresponding to different local rigidity values show that there is a significant connection between the stiffness of the substrate and the spreading of the cell. Cells that are on the stiffer side of the substrate show greater spread area and prominent actin network structure.

A quantitative analysis of the spread area of 3T3 fibroblast cells in relation to the stiffness of the substrate reveals that the spreading area of the cell increases considerably beyond a particular stiffness value of the substrate (Fig. 3b). Here, we found that on the comparably softer side of the substrate, where the stiffness value was in the range of 12–20 kPa, the cell spreading area increased very slowly from the value of  $(1570 \pm 730)$   $\mu\text{m}^2$  to  $(1900 \pm 1000)$   $\mu\text{m}^2$ . However, when the stiffness value changed from 20 to 50 kPa over the substrate's length, typically, the value of the cell spreading area increased from  $(1900 \pm 1000)$   $\mu\text{m}^2$  to  $(2700 \pm 1500)$   $\mu\text{m}^2$ . Furthermore, a statistical analysis of the variation of the cell shape with the stiffness of the substrate is shown in Fig. 3c. The circularity of the cell was taken into account to investigate the shape of the cell, which essentially measures the deviation from a rounded shape. The cells present on the softer side of the substrate were found to have near circular shape, and as the stiffness of the substrate increased significantly, the cells started to elongate (Fig. 3a). It was observed that when the stiffness of the substrate was in the range of 12–20 kPa, the circularity value of the cells was around  $(0.45 \pm 0.20)$ . However, when the stiffness of the substrate increased from a value of 20–50 kPa, the circularity of the cells started to decrease and reached around  $(0.38 \pm 0.20)$  on the stiffer side of the substrate.

The cytoskeletal organization of the cell is also altered in response to variations in the stiffness of the substrate (Fig. 4a–d). For cells on the softer part of the substrate ( $\approx 12$  kPa), there are no prominent actin stress fibers and same is the case for focal adhesions (Fig. 4a). However, as the substrate becomes stiffer, the cell's cytoskeleton becomes more organized, more filamentous actin start appearing, and focal adhesions start becoming more prominent (Fig. 4b–d). At the stiffer end of the substrate ( $\approx 50$  kPa), the actin stress fibers of the cells become more prominent and longer in length. In addition to that, the number of focal adhesion sites in cells increases. Therefore, it clearly indicates that the cells are more likely to stick to a substrate as its stiffness increases. Previous studies have documented that the cytoskeletal organization of cells and the spread of cells can vary with the stiffness of the substrate [1, 22, 26]. Our study captures all the essence of cellular mechanosensing as far as rigidity is concerned, in a single and continuous substrate.

## 4 Conclusion

Using a simple procedure of mixing hydrogels of different stiffness, we have demonstrated a simple yet effective way of producing stiffness gradient. Several studies have elucidated the rigidity sensing of cells using adhered cells on substrates with different rigidities. These substrates can be easily functionalised and used as a test substrate

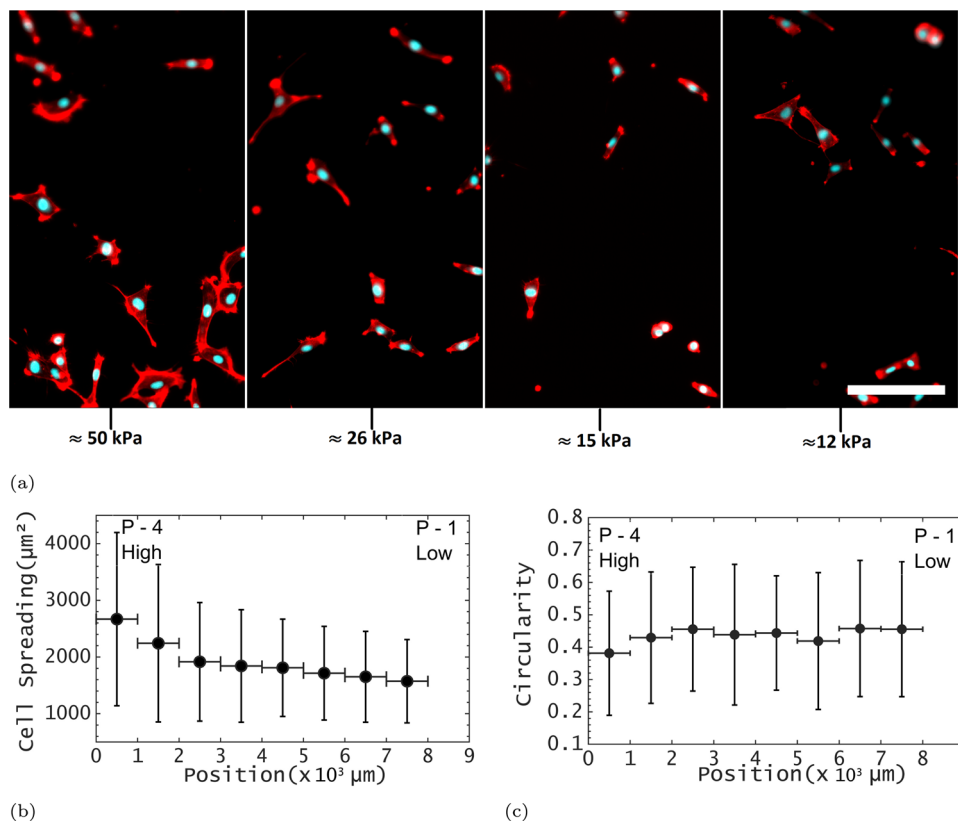


**Fig. 3** Cell area and cell shape distribution on gradient substrate: **a** Superimposed fluorescence image of 3T3 fibroblast cells on the fibronectin-coated rigidity-gradient hydrogel. Cell nuclear DNA was stained with DAPI (cyan) and f-actin was stained with phalloidin (red). The numerical value indicated on the lower side of each panel corresponds to an estimated measure of rigidity for various positions on the substrate. **b** Quantitative analysis of the relationship between substrate stiffness and cell spreading. Cell spreading is roughly constant at the lower stiffness side of the substrate and varies significantly along the substrate's stiffness variation on the higher stiffness side of the substrate. **c** Analysis of the cell shape (circularity) in relation to the substrate's stiffness variation, as the stiffness of the substrate increased, cells became elongated. Scale bar = 200  $\mu\text{m}$  and error bars along  $y$ -axis represent standard deviation; error bars along  $x$ -axis depict the size of the bin

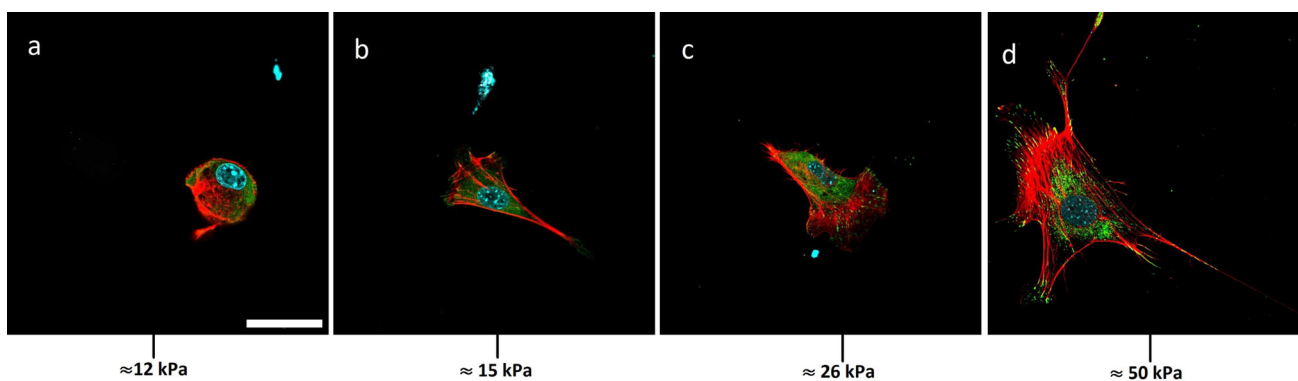


**Fig. 4** Actin-cytoskeleton organization along the rigidity-gradient substrate: 3T3 fibroblast cells nuclei are stained with DAPI (blue), cells f-actin stain with phalloidin (red) and focal adhesion of cells stain with vinculin (green). The number mentioned on the bottom side of individual panels represents the approximate rigidity value of different position on the substrate. Scale bar = 50  $\mu\text{m}$

for the investigation of cellular durotaxis. In this work, we have shown the response of the cells to various rigidities using a single substrate. As evident from the literature, different cells have affinity for a particular range of substrate rigidity. The substrate presented here can in principle be used for separating a cluster of cells on the basis of their affinity for a typical rigidity range. Furthermore, we also find the evidence of a threshold value of rigidity beyond which the cellular response becomes more prominent. We hypothesize that both the rigidity and the rigidity-gradient values are crucial determinants of cell's mechanical response.

**Supplementary Information** The online version contains supplementary material available at <https://doi.org/10.1140/epjs/s11734-024-01125-2>.

**Acknowledgements** Confocal microscopy was performed at the central instrumentation facility of the Indian Institute of Technology Palakkad. The project was supported by funding from the Indian Institute of Technology, Palakkad (ERG Grant-2023-161-PHY-BRS-ERG-SP).

## Author contribution statement

BRS designed the project. IB, SS, NM, and BK performed the experiments. All authors participated in the data analysis. IB, SS, BK, and BRS wrote the paper.

**Data availability** Data used in this work are available on demand.

## Declarations

**Conflict of interest** The authors declare no conflict of interest.

## References

1. T.A. Ulrich, E.M. de Juan Pardo, S. Kumar, The mechanical rigidity of the extracellular matrix regulates the structure, motility, and proliferation of glioma cells. *Cancer Res.* **69**(10), 4167–4174 (2009)
2. A.J. Engler, S. Sen, H.L. Sweeney, D.E. Discher, Matrix elasticity directs stem cell lineage specification. *Cell* **126**(4), 677–689 (2006)
3. R. McBeath, D.M. Pirone, C.M. Nelson, K. Bhadriraju, C.S. Chen, Cell shape, cytoskeletal tension, and rhoa regulate stem cell lineage commitment. *Dev. Cell* **6**(4), 483–495 (2004)
4. D.E. Discher, P. Janmey, Y.-l Wang, Tissue cells feel and respond to the stiffness of their substrate. *Science* **310**(5751), 1139–1143 (2005)
5. G. Kulkarni, P.G. Ray, P.K. Byram, M. Kaushal, S. Dhara, S. Das, Tailorable hydrogel of gelatin with silk fibroin and its activation/crosslinking for enhanced proliferation of fibroblast cells. *Int. J. Biol. Macromol.* **164**, 4073–4083 (2020)
6. T. Luo, B. Tan, L. Zhu, Y. Wang, J. Liao, A review on the design of hydrogels with different stiffness and their effects on tissue repair. *Front. Bioeng. Biotechnol.* **10**, 2296–4185 (2022)
7. T. Yeung, P.C. Georges, L.A. Flanagan, B. Marg, M. Ortiz, M. Funaki, N. Zahir, W. Ming, V. Weaver, P.A. Janmey, Effects of substrate stiffness on cell morphology, cytoskeletal structure, and adhesion. *Cell Motil. Cytoskelet.* **60**(1), 24–34 (2005)
8. T.A. Ulrich, E.M. de Juan Pardo, S. Kumar, The mechanical rigidity of the extracellular matrix regulates the structure, motility, and proliferation of glioma cells. *Cancer Res.* **69**(10), 4167–4174 (2009)
9. M. Gupta, B.R. Sarangi, J. Deschamps, Y. Nematbakhsh, A. Callan-Jones, F. Margadant, R.-M. Mège, C.T. Lim, R. Voituriez, B. Ladoux, Adaptive rheology and ordering of cell cytoskeleton govern matrix rigidity sensing. *Nat. Commun.* **6**(1), 7525 (2015)
10. C.-M. Lo, H.-B. Wang, M. Dembo, Y.-l Wang, Cell movement is guided by the rigidity of the substrate. *Biophys. J.* **79**(1), 144–152 (2000)
11. H. Cao, L. Duan, Y. Zhang, J. Cao, K. Zhang, Current hydrogel advances in physicochemical and biological response-driven biomedical application diversity. *Signal Transduct. Target. Ther.* **6**(1), 426 (2021)
12. J.P. Joseph, N. Gupta, C. Miglani, D. Nath, A. Singh, D. Gupta, A. Pal, Unraveling on-demand strain-stiffening in nanofibrous peptide-polymer conjugates to mimic contractility in actinomyosin networks. *Chem. Mater.* **34**(10), 4364–4374 (2022)
13. V. Girdharan, Y. Yun, P. Hajdu, L. Conforti, Microfluidic platforms for evaluation of nanobiomaterials: a review. *J. Nanomater.* **2012**, 1–14 (2012)
14. J.A. Burdick, A. Khademhosseini, R. Langer, Fabrication of gradient hydrogels using a microfluidics/photopolymerization process. *Langmuir* **20**(13), 5153–5156 (2004)
15. D. Lee, K. Golden, M.M. Rahman, A. Moran, B. Gonzalez, S. Ryu, Fabrication of hydrogels with a stiffness gradient using limited mixing in the hele-shaw geometry. *Exp. Mech.* **59**, 1249–1259 (2019)



16. F.C. Sales, R.M. Ariati, V.T. Noronha, J.E. Ribeiro, Mechanical characterization of pdms with different mixing ratios. *Procedia Struct. Integr.* **37**, 383–388 (2022)
17. J.R. Tse, A.J. Engler, Preparation of hydrogel substrates with tunable mechanical properties. *Curr. Protoc. Cell Biol.* **47**(1), 10–16 (2010)
18. S. Syed, A. Karadaghy, S. Zustiak, Simple polyacrylamide-based multiwell stiffness assay for the study of stiffness-dependent cell responses. *JoVE (J. Vis. Exp.)* **97**, 52643 (2015)
19. R. Sunyer, A.J. Jin, R. Nossal, D.L. Sackett, Fabrication of hydrogels with steep stiffness gradients for studying cell mechanical response. *PLoS ONE.* **7**(10), e46107 (2012)
20. M. Krieg, G. Fläschner, D. Alsteens, B.M. Gaub, W.H. Roos, G.J. Wuite, H.E. Gaub, C. Gerber, Y.F. Dufrêne, D.J. Müller, Atomic force microscopy-based mechanobiology. *Nat. Rev. Phys.* **1**(1), 41–57 (2019)
21. C.E. Kandow, P.C. Georges, P.A. Janmey, K.A. Beninger, Polyacrylamide hydrogels for cell mechanics: steps toward optimization and alternative uses. *Methods Cell Biol.* **83**, 29–46 (2007)
22. F.J. Byfield, Q. Wen, I. Levental, K. Nordstrom, P.E. Arratia, R.T. Miller, P.A. Janmey, Absence of filamin a prevents cells from responding to stiffness gradients on gels coated with collagen but not fibronectin. *Biophys. J.* **96**(12), 5095–5102 (2009)
23. S. Seiffert, W. Oppermann, Diffusion of linear macromolecules and spherical particles in semidilute polymer solutions and polymer networks. *Polymer* **49**(19), 4115–4126 (2008)
24. L. Haggerty, J.H. Sugarman, R.K. Prud'homme, Diffusion of polymers through polyacrylamide gels. *Polymer* **29**(6), 1058–1063 (1988)
25. W.J. Hadden, J.L. Young, A.W. Holle, M.L. McFetridge, D.Y. Kim, P. Wijesinghe, H. Taylor-Weiner, J.H. Wen, A.R. Lee, K. Bieback et al., Stem cell migration and mechanotransduction on linear stiffness gradient hydrogels. *Proc. Natl. Acad. Sci.* **114**(22), 5647–5652 (2017)
26. G. Jiang, A.H. Huang, Y. Cai, M. Tanase, M.P. Sheetz, Rigidity sensing at the leading edge through  $\alpha v \beta 3$  integrins and  $rpt\alpha$ . *Biophys. J.* **90**(5), 1804–1809 (2006)

Springer Nature or its licensor (e.g. a society or other partner) holds exclusive rights to this article under a publishing agreement with the author(s) or other rightsholder(s); author self-archiving of the accepted manuscript version of this article is solely governed by the terms of such publishing agreement and applicable law.